

Angular Dependence of Neutrino Flux in KM^3 Detectors in Low Scale Gravity Models

Pankaj Jain¹, Supriya Kar¹, Douglas W. McKay²
Sukanta Panda¹ and John P. Ralston²

¹Physics Department
I.I.T. Kanpur, India 208016

²Department of Physics & Astronomy
University of Kansas
Lawrence, KS 66045

Abstract: Cubic kilometer neutrino telescopes are capable of probing fundamental questions of ultra-high energy neutrino interactions. There is currently great interest in neutrino interactions caused by low-scale, extra dimension models. Above 1 PeV the cross section in low scale gravity models rises well above the total Standard Model cross section. We assess the observability of this effect in the 1 PeV - 1000 PeV energy range of kilometer-scale detectors, emphasizing several new points that hinge on the enhancement of neutral current cross sections with respect to charged current cross sections. A major point is the importance of “feed-down” regeneration of upward neutrino flux, driven by new-physics neutral current interactions in the flux evolution equations. Feed-down is far from negligible, and it is essential to include its effect. We then find that the angular distribution of events has high discriminating value in separating models. In particular the “up-to-down” ratio between upward and downward-moving neutrino fluxes is a practical diagnostic tool which can discriminate between models in the near future. The slope of the angular distribution, in the region of maximum detected flux, is also substantially different in low-scale gravity and the Standard Model. These observables are only weakly dependent on astrophysical flux uncertainties. We conclude that angular distributions can reveal a breakdown of the Standard Model and probe the new physics beyond, as soon as data become available.

1 Introduction

The Ultra-high energy neutrino nucleon cross section $\sigma_{\nu N}$ is a topic of fundamental physical importance. Low scale gravity models [1, 2] predict enhancement of the neutrino-nucleon neutral current type cross section at center of mass energies above the fundamental gravity scale of about 1 TeV [3, 4, 5].¹ Consequences for cosmic ray physics have been studied in application to the highest energy cosmic rays [3, 4, 5, 6, 7, 8, 9, 10, 11], where there is great interest in possible violation of the Greisen, Zatsepin, Kusmin (GZK) bound [12], at roughly 10 EeV ($10^{19}eV$). There is also great interest in application to an intermediate range [5, 13, 14], roughly 0.1 - 100 PeV ($10^{14} - 10^{17} eV$). The history and future of the highest energy experiments [15] and intermediate energy experiments [16] provide a tremendous impetus for these studies pointing toward new physics.

Whatever the model, there are rich opportunities to study fundamental high energy interactions by focusing on (1) the ratio of neutral current type events to charged current events and (2) the *angular distribution* of events in upcoming experiments. The neutral-to-charged ratio and the angular distribution shape do not depend on the uncertainties of overall flux normalizations. The primary uncertainty in all cosmic ray comparisons with theory – the overall scale of the flux – drops right out. For a range of models with standard and reasonable flux spectral indices, the angular distributions are also remarkably *insensitive* to the details of the model. The strongest determining factor in the shape of the angular distribution is the fundamental physics of the interaction cross section itself. We emphasize and explore this fact, showing that arrays now planned or under construction could stringently test the Standard Model and proposals for new physics simply on the basis of the neutral-to-charge ratio and the *slope* of the angular distribution of neutrino-nucleon events. In the context of extra space-time dimensions, data could determine or bound such details as the scale and number of extra dimensions in the present models.

Here we continue earlier work [5] that examined possible signatures of enhanced $\sigma_{\nu N}$ in kilometer scale detectors. Extensions of the currently operating AMANDA [17] and RICE [18, 19] experiments to ICECUBE [20]

¹In the present context, by neutral current type cross section we mean there is no leading, charged lepton produced. The shower is essentially hadronic, which includes the case of black hole final states.

dimensions would certainly explore the 1 PeV - 100 PeV region. In the case of RICE, modest improvements even allow a reach above the EeV range. In [5] we used a linear extrapolation of the low scale gravity mediated neutral current $\sigma_{\nu N}$ from the low energy, $\sqrt{s} \ll 1$ TeV, region, to the $\sqrt{s} \geq 1$ TeV region and found a very sharp suppression of the up-to-down ratio compared to the standard model that set in at about 5 PeV for $M = 1$ TeV and at about 50 PeV for $M = 2$ TeV.

In that earlier study [5], we did not apply other extrapolations of the cross section to the up-to-down calculation, nor did we include the “feed down” effect [21, 22], which results from neutral current interactions degrading higher energy neutrinos as they travel through the earth and “feeding” the flux at lower energies. In the standard model, this effect is small above 1 PeV where the flux decrease steepens and the neutral current cross section is too small to compensate. In contrast, this effect turns out to be extremely important after including the gravity induced neutral current $\sigma_{\nu N}$, which rises rapidly with energy. This point has not been explicitly recognized previously in connection with gravity enhancement.

A number of new gravity effects relevant to energies above the fundamental scale, applicable to physics at the Large Hadron Collider (LHC), kilometer cubed detectors (KM^3) and GZK energies, have been proposed recently. In both Arkani-Hamed, Dimopoulos and Dvali (ADD) [1] and Randall and Sundrum (RS) [2] models, eikonal treatment of the effective low energy amplitude (used as the “Born term” input) has been studied [23] and applied to LHC [24] and GZK [8] energies. In string realizations of the ADD framework [25], “stringy” cross sections, relevant just below M , have been estimated [26, 27, 28], as has the black hole formation cross section [29, 7], which may be relevant above M , including the GZK energy region. We have investigated all of these options, and find that the eikonalized ADD low energy “Born amplitude” and “geometrical” black hole cross sections lead to the largest and least model dependent effects in our 1 PeV to 1000 PeV KM^3 application.² Our study goes beyond that reported recently in [13] in two respects: we emphasize higher energies and we include and analyze the consequences of the new, eikonalized graviton exchange component of the neutral current interaction. This latter point also distinguishes our work from a recent black hole detection study [14].

²We do not treat the possibility of brane production and decay here [30].

We should note here that, though the neutral current does not produce a prompt electron shower or leading muon characteristic of charged current signatures, one expects that the hadronic shower, which is completely electromagnetic after several radiation lengths, will be an observable signature of neutral current interactions. For this reason we regard all of the current detection mechanisms to be relevant to our study, certainly including RICE, which can detect a radio pulse from any kind of shower, AMANDA and ICECUBE.

1.1 The Cross Section

At C.M. energies well above the Planck mass, the classical gravity Schwarzschild radius $R_s(\sqrt{s})$ is the dominant physical scale. The classical impact parameter, b , may make sense in this domain, and the eikonal approximation be valid, for values of b larger than R_s . We will sketch the eikonal set-up shortly. At smaller impact parameters, the parton-level geometrical cross section

$$\hat{\sigma}_{BH} \approx \pi r_S^2 \quad (1)$$

provides a classical, static estimate of the cross section to form black holes. In Eq. 1 r_S is the Schwarzschild radius of a $4 + n$ dimensional black hole of mass $M_{BH} = \sqrt{\hat{s}}$,

$$r_S = \frac{1}{M} \left[\frac{M_{BH}}{M} \right]^{\frac{1}{1+n}} \left[\frac{2^n \pi^{(n-3)/2} \Gamma\left(\frac{3+n}{2}\right)}{2+n} \right]^{\frac{1}{1+n}} \quad (2)$$

where $\sqrt{\hat{s}}$ is the parton-parton or, in our case, neutrino- parton C.M. energy, and M is the $4+n$ -dimensional scale of quantum gravity.³ The black hole production process is expected to give a dominant contribution when $\sqrt{\hat{s}} \gg M$. Black holes will form only if the impact parameter $b < r_S$. To convert Eq.1 into an estimate for the neutrino- nucleon cross-section, we fold it with with the sum over parton distribution functions and integrate over x -values, where $\hat{s} = xs$, at a momentum transfer typical of the black hole production process:

$$\sigma_{\nu N \rightarrow BH}(s) = \sum_i \int_{x_{min}}^1 dx \hat{\sigma}_{BH}(xs) f_i(x, q). \quad (3)$$

³We use the mass scale convention discussed in [10], referred to as M_D there.

Black hole formation requires $x > M^2/s$, so we take $x_{min} = M^2/s$. In addition, $q^{-1} = b < r_S$ is required. We adopt $q = \sqrt{\hat{s}}$ up to $\sqrt{\hat{s}} = 10TeV$, the maximum range in q of the CTEQ parton distribution functions [31], the set we use, and $q = 10TeV$ when $\sqrt{\hat{s}}$ is above this value. As remarked in [10], the dependence of $\sigma_{\nu N \rightarrow BH}(s)$ on the choice of x_{min} and the treatment of q is rather mild.

In the case of ADD model the black hole production cross sections can be large for $n > 2$, in which case the fundamental scale can be of the order of 1 TeV. A number of authors have adopted this estimate and applied it to ultra relativistic, parton level scattering. The approximation has been challenged on the basis that quantum corrections should lead to exponential suppression of individual channels, such as the black hole formation final state [32, 33], with several, independent arguments advanced in each case. In defense of the ‘‘black disk’’ approximation, several authors also point to success of internal consistency checks of the classical picture [28, 34, 24]. Recent phenomenological studies seem to be agnostic on this issue [9, 10, 11, 14, 35], treating the phenomenological consequences of both versions.

In a string picture with scale $M_s < M$, there is a range of energy $M_s \simeq \sqrt{s}$ where string resonances dominate [26], and a range $M_s < \sqrt{s} \leq M$, where stringball formation [28] could dominate.⁴ The cross section can be roughly expressed as [26]

$$\sigma_{SR}(\sqrt{s}) \sim g_s^2 \delta(s - M_{SR}^2), \sqrt{s} \simeq M_{SR}, \quad (4)$$

for the string resonance case. Here g_s is the (weak) string coupling constant and M_{SR} is the mass of a string resonance state. Similarly, for the stringball case, estimates of the cross section give [28]

$$\sigma_{SB}(\sqrt{s}) \sim 1/M_s^2, M_s/g_s < \sqrt{s} < M_s/g_s^2, \quad (5)$$

where M is a few times less than M_s/g_s^2 for weak coupling. The impact of these various processes on the physics to be expected at the LHC, at a next linear collider (NLC) and very large hadron collider (VLHC) has been surveyed in a number of papers, summarized and referenced in the Snowmass 2001 report of the extra dimensions subgroup [36].

⁴In this discussion we suppress the \hat{s} notation for convenience, though parton level processes are intended.

In our application to KM^3 physics in this paper, we mentioned above that the “classical” eikonal cross section [37, 23] and the geometric black hole formation cross section are the only cases where we find potentially observable effects. We outline our treatments of the eikonal model in the ADD [1] and RS1 [2] pictures next. The black hole cross section needs no further elaboration. The fundamental mass scale M in the case of the ADD model for $n > 2$, can be of the order of 1 TeV, though new astrophysics analyses may constrain $n = 3$ more severely, as we comment below [38]. Similarly, in the RS picture the effective scale of gravity on the physical brane, the lowest K-K mode mass, can be arranged to be of the order of 1 TeV. In all of our quantitative work, we set the scale M the same for every value of n we use in our comparisons. As noted earlier, the scale M is the same as M_D defined in [24] and discussed in [10].

In the RS1 model with one extra dimension or in the ADD model with several, a possible choice for the input amplitude to the eikonal approximation, referred to as the Born amplitude, is given by,

$$i\mathcal{M}_{\text{Born}} = \sum_i \frac{ics^2}{M^2} \frac{1}{q^2 + m_i^2} \quad (6)$$

where c is the gravitational coupling strength, which is effectively Newtonian for ADD and electroweak for RS. Here $q = \sqrt{-t}$ is the momentum transfer. In the Randall-Sundrum case, the sum runs over the massive K-K modes, constrained to start at or above the TeV scale when c is of order electroweak strength. Their spacing is then also of TeV order. In the ADD case, the index i must include the mass degeneracy for the i th K-K mode mass value. The spectrum is so nearly continuous that an integral evaluation of the sum is valid, but must be cut off at a scale generally taken to be of the order of M . Taking the transverse Fourier transform of the Born amplitude, we get the eikonal phase as a function of impact parameter, b ,

$$\chi(s, b) = \frac{i}{2s} \int \frac{d^2q}{4\pi^2} \exp(i\mathbf{q} \cdot \mathbf{b}) i\mathcal{M}_{\text{Born}} \quad (7)$$

For the ADD model, where $c = (M/\overline{M}_P)^2$ and $\overline{M}_P = 2.4 \times 10^{18}$ GeV is the reduced, four dimensional Planck mass,

$$\chi(s, b) = -\frac{s(2^{2n-3}\pi^{\frac{3n}{2}-1})}{M^{n+2}\Gamma(n/2)} 2 \int_0^\infty dmm^{n-1} K_0(mb)$$

$$= \left(\frac{b_c}{b} \right)^n, \quad (8)$$

where

$$b_c^n = \frac{1}{2}(4\pi)^{\frac{n}{2}-1} \Gamma\left[\frac{n}{2}\right] \frac{s}{M^{2+n}}. \quad (9)$$

Because of the exponential decrease of K_0 , the phase integral is actually ultraviolet finite. For the RS model, the corresponding expression is

$$\chi(s, b) = \sum_i \frac{cs}{2M^2} K_0(m_i b). \quad (10)$$

For widely spaced KK modes in the Randall-Sundrum case, the lowest few modes dominate and contribute insignificantly in the $1 \text{ PeV} < E_\nu < 100 \text{ PeV}$ region. We do not discuss RS further.

The eikonal amplitude is then given in terms of the eikonal phase by

$$\begin{aligned} \mathcal{M} &= -2is \int d^2b \exp(i\mathbf{q} \cdot \mathbf{b}) [\exp(i\chi) - 1] \\ &= -i4\pi s \int db b J_0(qb) [\exp(i\chi) - 1], \end{aligned} \quad (11)$$

The eikonal amplitude for the case of ADD model can be obtained analytically [23, 8, 24] in the strong coupling $qb_c \gg 1$ and weak coupling $qb_c \ll 1$ regimes.

In the strong coupling regime the eikonal amplitude can be computed using the stationary phase approximation and is given by,

$$\mathcal{M} = A_n e^{i\phi_n} \left[\frac{s}{qM} \right]^{\frac{n+2}{n+1}}, \quad (12)$$

where

$$A_n = \frac{(4\pi)^{\frac{3n}{2(n+1)}}}{\sqrt{n+1}} \left[\Gamma\left(\frac{n}{2} + 1\right) \right]^{\frac{1}{1+n}}, \quad (13)$$

$$\phi_n = \frac{\pi}{2} + (n+1) \left[\frac{b_c}{b_s} \right]^n \quad (14)$$

and $b_s = b_c(qb_c/n)^{-1/(n+1)}$. In the weak coupling regime, $q \rightarrow 0$ the amplitude is given by

$$\mathcal{M}(q=0) = 2\pi i s b_c^2 \Gamma\left(1 - \frac{2}{n}\right) e^{-i\pi/n}. \quad (15)$$

As it turns out, the small q region contributes little to the cross section, and we use the simple rule that the amplitude is set to its value at $q = 1/b_c$ for values $q \leq 1/b_c$.

The parton-level cross section is calculated by assuming that it is given by the Born term as long as $\hat{s} < M^2$. For $\hat{s} > M^2$ the cross section is estimated by the eikonal amplitude.⁵ For $M = 1$ TeV, for example, the actual matching between the Born and eikonal amplitudes occurs in the range $\sqrt{\hat{s}} = 1 - 3$ TeV, depending on n and the value of $y = q^2/\hat{s}$. In any case the region $\sqrt{\hat{s}} \sim M$ contributes negligibly to the cross-section, so the precise matching choice makes no difference in the final result. The eikonal calculation is not expected to be reliable if the momentum transfer $q > M$. At large momentum transfer we assume that the black hole production dominates the cross section. The eikonal cross section is, therefore, cut off once the momentum transfer $q > 1/r_S$. The neutrino-parton differential cross-section is folded with the CTEQ parton distributions and integrated over x and y variables, consistent with our momentum transfer restriction on the eikonal amplitude. The CTEQ limit at $x = 10^{-5}$ is exceeded only at the high end of the energy range we study. A standard power law extrapolation is used when x does range below this value, though the \hat{s} values are so low that the contribution of this range to the cross section is negligible. In Fig. 1 we plot the total neutrino-nucleon cross sections for several different values of the fundamental scale M and the number of extra dimensions n , including both eikonal and black hole production contributions. The cross section is clearly more sensitive to the choice of the scale parameter, M , than to the number of dimensions, n . In fact the sensitivity to choice of n comes primarily through the dependence of the differences in bounds on M corresponding to different choices of n . The strongest bounds on M come from astrophysical and cosmological considerations, which unavoidably require some degree of modeling.

A recent review of experimental and observational constraints is given in [38], where lower bounds on M are quoted for $n = 3$ from various analyses such as supernova cooling, regarded as the least model dependent bound ($M \geq 2.5TeV$), post-inflation re-heating ($M \geq 20TeV$), and neutron star heat excess ($M \geq 60TeV$). For $n = 4$, the most severe constraint is $M \geq$

⁵A discussion of the reliability of the eikonal amplitude in the $5 \text{ TeV} \leq \sqrt{s} \leq 15 \text{ TeV}$ range is given in [24].

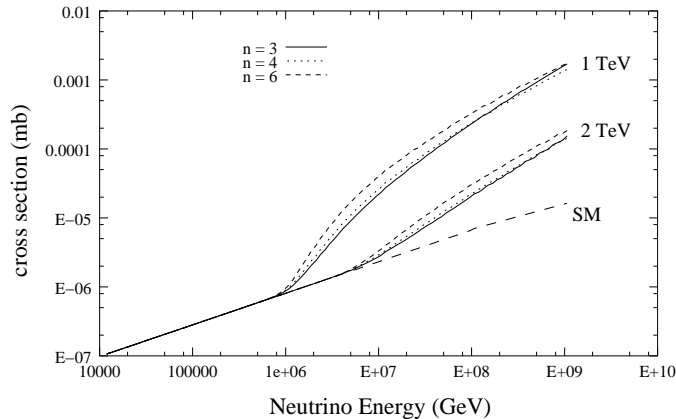


Figure 1: The neutrino-proton cross section $\sigma_{\nu p}$ in the ADD model using the number of extra dimensions $n = 3, 4, 6$ as a function of the neutrino energy E_ν for $E_\nu < 10^8$ GeV. The geometric black hole production cross section is included. The solid, dotted and short dashed curves correspond to $n = 3, 4$ and 6 respectively. The long dashed curve represents the Standard Model prediction.

5TeV in the case of the post-inflation re-heating limit. There are essentially no constraints on the cases $n = 5$ and 6 . Laboratory lower bounds are typically of order 1 TeV or less for all $n \geq 2$, with LEP II providing the strongest bound at 1.45 TeV for $n=2$.

2 Event Rates of Downward Neutrinos

In Fig. 2, we show the downward event rate, defined as the number of interactions from down-coming neutrinos, within a one kilometer cubed volume. We use two, quite different input flux assumptions to show the dependence of rate on the flux. A simple parameterization of an optically thick source model of flux above 1 PeV given in Ref. [39] (SDSS) is used, along with the flux bound for optically thin source environments of Ref. [40] (WB). The flux in [39] is about two orders of magnitude larger than the bound in [40], and it has roughly an E^{-2} power law behavior from 0.1 PeV

to 10 PeV, and then it steepens to approximately E^{-3} . We parametrized the SDSS flux such that it falls as E^{-2} for $10 \text{ TeV} < E < 10 \text{ PeV}$ and as E^{-3} for $E > 10 \text{ PeV}$. The WB bound, on the other hand, falls as E^{-2} over the whole energy range. The two flux curves cross at about 10^3 PeV .

Our estimate is made by taking the vertical flux result, multiplying it by 2π steradians and by the probability that a neutrino would interact within 1 km in ice, with density 0.93 gm/cc, given the cross section model in question. To get an actual event rate for a given detector, we would have to multiply by the acceptance of the detector. In the SDSS flux model, Fig. 2a, the number of interactions peaks at around 10 PeV for the $M = 1 \text{ TeV}$ case, with encouragingly large numbers of interactions, in the 350-650 range, induced by low-scale gravity. This is 10-20 times the SM interaction rate at the same energy. The number and the location of the peak rate depend upon the flux model of course [22]. This dependence is illustrated in Fig. 2b, where the event rate for the WB bound is shown. The event rates are lower by a factor of about 50 and the gravity induced events have a much broader peak, centered at about 15 PeV, compared to the SDSS case. The peak is broader for the WB flux than for SDSS because the WB limit falls as E^{-2} throughout this energy region, while the SDSS flux falls as E^{-3} above 10 PeV, cutting off the higher energy events more rapidly. The shape of the SM event rate is the same in both cases, since the flux shapes are the same below 10 PeV.

The excess above the SM is roughly half neutral current type events arising from eikonized graviton exchange and half black hole events, which decay predominantly into hadrons. Therefore an optimal detection scheme requires sensitivity to the hadronic shower from the deposited energy in the ice. The ICECUBE and RICE detectors, for example would respond readily to hadron showers at these energies. The special role of enhanced neutral current type events, those with hadronic signatures like the graviton exchange and black hole events, prompts us to propose that the ratio of neutral current to charged current events provides a powerful tool to uncover new interactions. In particular, if the neutral current type component, distinguished by hadronic dominated showers and no leading charged lepton, *dominates*, as it does in the black hole and the eikonal regimes of the low scale gravity models, there would be *no standard model explanation*. The ratio of neutral current type events to charged current events, distinguished by the presence of a leading charged lepton, is shown in Fig.3. The rapid rise that sets in above the threshold for new physics is remarkable, and would be so even without

the black hole contribution. Even scales $M > 2TeV$ are discernible with this observable. Putting together the information from several techniques, RICE and ICECUBE for example, one might well separate the “neutral” versus “charged” character of events and find a clear window on new physics.

3 The Regeneration and Angular Dependence of Neutrino Flux

We next calculate the up over down ratio of neutrino flux. The downward $\phi_0(E_\nu)$ is the flux of neutrinos incident on the surface of the earth from the sky. We will consider only the diffuse neutrino flux and assume that it is isotropic. Our calculations are easily generalized if the flux is found to be non-isotropic or if we are interested in individual sources. The upward flux $\phi_{\text{up}}(E_\nu)$ is defined as the flux of neutrinos coming upwards from the surface of the earth. This is the angular average

$$\phi_{\text{up}}(E_\nu) = \frac{1}{2\pi} \int_0^{2\pi} d\Phi \int_0^{\pi/2} \sin(\theta) d\theta \phi(E_\nu, \theta) \quad (16)$$

of the flux $\phi(E_\nu, \theta)$ emerging from the earth, where θ is the polar angle with respect to the nadir and Φ is the azimuthal angle. The ratio R is essentially the ratio of up-to-down event rates. The event rates are given by the product of flux, cross section, number density, volume and acceptance, and to the extent that the latter four factors cancel in the ratio, only the up-to-down ratio of fluxes survives. This ratio is affected by the energy dependence of the flux, but not to its overall normalization. The upward flux depends on the cross sections of course, as we elaborate next.

In order to determine $\phi(E_\nu, \theta)$ we first need to solve the *evolution equation* for the neutrino propagating through the interior of the earth. In the case of the standard model, the neutrino cross section is dominated by the charged current, the neutral current does little to evolve, or “feed down”, the rapidly falling flux above 1 PeV, and neutrinos basically get lost after collision inside earth. In the present case, on the other hand, the eikonized graviton exchange gives a large contribution to the feed down above 1 PeV, and we have to include this important enhancement of regeneration of lower

energy neutrinos from higher energy.^{6 7} The large cross sections mean that neutrinos experience many interactions as they proceed through the earth, even at angles near the horizon. For instance, just 5 degrees below the horizon a 100 PeV neutrino traverses more than 20 interaction lengths of earth before reaching the detector region. This behavior supports our use of the continuous evolution model, summarized below in Eq.17, since fluctuations are small for UHE application, where the cross section is large. The neutrino loses little energy during any particular collision and hence it is reasonable to assume that it practically moves in a straight line path. The evolution equation for the neutrino is given by [21, 22]

$$\begin{aligned} \frac{d \ln \phi}{dt}(E_\nu, \theta) &= -\sigma_{W+BH}^{\nu N}(E_\nu) - \sigma_{Z+E}^{\nu N}(E_\nu) + \int_{E_\nu}^{\infty} dE' \frac{\phi(E', \theta)}{\phi(E_\nu, \theta)} \frac{d\sigma_{Z+E}^{\nu N}(E', E_\nu)}{dE'} \\ &\equiv -\sigma_{\text{eff}}^{\nu N}(E_\nu, \theta), \end{aligned} \quad (17)$$

where $\sigma_{W+BH}^{\nu N}$ is the “neutrino absorbing” W-exchange + black hole cross section and $\sigma_{Z+E}^{\nu N}$ is the “neutrino regenerating” Z-exchange + eikonalized graviton exchange cross section. In Eq.17, $dt = n(r)dz$ and $n(r)$ is the number density of nucleons at any distance r from the center of earth, radius R_e . Expressing the flux $\phi(E_\nu, \theta)$ as

$$\phi(E_\nu, \theta) = \phi_0(E_\nu) \exp[-\sigma_{\text{eff}}(E_\nu, \theta)t(\theta)], \quad (18)$$

where the column density at upcoming angle of entry θ , chord length $2R_e \cos \theta$, is given by

$$t(\theta) = \int_0^{2R_e \cos \theta} n(z, \theta) dz, \quad (19)$$

we solve equations 17 and 18 numerically by iteratively improving the flux $\phi(E_\nu, \theta)$. Using this solution we can determine the ratio R of up to down flux,

$$R = \frac{\phi_{\text{up}}(E_\nu)}{\phi_0(E_\nu)} \quad (20)$$

⁶The black hole production component, in contrast, essentially leads to loss of neutrinos upon collision. In the present context, the black hole interaction acts like the charged current in the standard model. The eikonal component has the character of the usual neutral current, transferring a small fraction of the neutrino energy to the hadron and leaving a leading neutrino in the final state.

⁷We do not treat the regeneration of τ neutrinos through τ production by ν_τ and subsequent τ decay back to ν_τ [41].

By using R , one sharply reduces the effects of experimental systematics and flux normalization and isolates the dependence on cross sections and flux shape. Refinements of angular binning can add information according to the size of the data sample, as we discuss below.

In Fig. 4 we plot the ratio R as a function of the neutrino energy. This figure illustrates two points: the ratio R is insensitive to the normalization of the flux assumed and, given a flux, the feed-down from higher to lower energies as the neutrinos pass through the earth is a powerful effect. In this application, our two, quite different input flux assumptions, show the *insensitivity* of R to the flux used. The long dashed curve gives the ratio for the larger flux with a “knee” from [39], while the shorter dashed line gives the result of the smaller flux bound with uniform E^{-2} fall-off of [40]. The solid curve refers to the SM cross section input, the two flux models give indistinguishable results in this case and are shown as one line. The lowest curve shows the ratio as a function of energy with pure absorption, in the sense that only the first two terms in σ_{eff} , Eq.17., are included. The two flux models give the same result, as they should. The sum of the eikonal and black hole cross section is used, the eikonal providing the neutral-current cross section and the black hole the purely absorptive cross section, as described in footnote 6. The cross section are computed in the ADD model, and the value $n = 3$ and the scale of quantum gravity $M = 1$ TeV. We see that the regeneration term gives a big effect for $M = 1$ TeV, producing factors of more than 10 above 20 PeV, and it is essential to include it in assessing the consequences of the low scale gravity models. Though radically different from each other, the two flux assumptions lead to nearly identical values of R out to 50 PeV and then differ only weakly above that, where the effect of the steeper decrease of SDSS flux shows up.

In Fig. 5 we plot the results for the ratio R in the ADD model as a function of the neutrino energy for the choice of the fundamental scale $M = 1, 2$ TeV and the number of extra dimensions equal to 3,4 and 6. The result depends on both the number of extra dimensions and, especially strongly, on the fundamental scale M . If the fundamental scale is larger than about 2 TeV, the KM^3 neutrino detectors will not be able to distinguish the Standard model result from the predictions of quantum gravity by using R as a diagnostic. However for $M \approx 1$ TeV, we find that the effect is very large and, given enough flux, could be seen in these detectors. For energies above 1 PeV, a noticeable difference in R between the two cases is seen. With

sufficient data, a distinction between no deviation from the standard model and a deviation corresponding to $M = 1$ with $n = 3, 4$ or 6 may be drawn.

The angular distribution of upward flux is an important diagnostic tool, as we stressed in the Introduction. In Fig. 6, we show the integrated flux per square kilometer per year above 1.8 PeV as a function of nadir angle for $M = 1, 2$ and $n=3,4,6$. The (higher) 2 TeV curve is essentially the same as for the SM, while the (lower) curves for $M = 1$ show clear suppression at all nadir angles up to $\pi/2$. It is somewhat disguised by the log scale, but most of the contribution to the ratio R comes from the highest event rates near the horizontal. With several bins of good statistics data above 1 radian in nadir angle, one can distinguish the slopes of the flux vs. nadir angle near the horizontal. The difference between these slopes for the SM and low scale gravity models when $M \simeq 1TeV$ provides another new physics discriminator. As in the case of the R observable, the slope is insensitive to the flux *value*, enhancing its power at identifying the nature of the neutrino *interactions*.

Realistically, one needs enough upcoming events at a given energy to calculate a meaningful ratio. The situation for the two flux models we are discussing is shown in the table.

		Number of upward events per year			
n	M	1-10 PeV	5 - 10 PeV	> 10 PeV	> 15 PeV
3	1	83	7.2	1.3	0.22
4	1	79	5.4	0.62	0.07
6	1	74	2.6	0.09	0.004
3	2	80	8.9	4.3	1.8
4	2	80	8.9	4.2	1.7
6	2	80	9	4.1	1.6
SM		80	8.8	4.2	1.7

Table 1: The numbers of upward events per year expected over the energy ranges shown, for models with different n and M choices and for the standard model. The flux used is our rough approximation to SDSS above 1 PeV

For our two power law approximation to the flux of [39] (SDSS), we see from the table that there are enough events with $E_\nu > 10$ PeV in a 10 year run to determine the ratio R . Can one discriminate among the different physics models for the cross section with the events? Fig. 5 shows that

if there are enough upcoming events to calculate a meaningful value for R , there are clear distinctions among the models. For example, taking a naive, purely statistics estimate, the $M = 1$ TeV, $E_\nu > 10$ PeV case would produce 13 ± 3 , 6 ± 2 and 1 ± 1 events for $n = 3, 4$ and 6 . Combining these values with the downward event rates (see Fig. 2), we see that the distinction between the $n = 3$ case and the $n = 6$ cases is significant. When $M = 2$ TeV, the numbers of upcoming events is essentially the same for the low scale gravity models and the SM. In 5 - 10 years of data, there would be enough events to determine an up-to-down ratio reasonably well. Figure 2 shows that the number of downward events is larger in the low scale gravity models than in the SM, because of their larger cross sections, so R values are different for the different cases. Thus, even for $M = 2$, values of R above 15 PeV are distinctly different in the two classes of models, as one sees in Fig. 5. In fact, within the low scale gravity models themselves there is more than a factor two difference between $n = 3$ and $n = 6$. Moreover, the low scale gravity models can all be easily distinguished from the SM with 5 years of data, with the number of events per year shown in the table. Even the cut > 15 PeV allows the meaningful distinction between the low scale models and the SM in 5 - 10 years of data. Using the WB bound on the optically thin source flux, we find that the upward events are too sparse to discriminate among models by use of the R ratio. Flux values in between the two presented here offer various levels of discrimination, with useful information obtainable for the larger fluxes.

Putting together the rise in downward event rate above 1 PeV, the sensitivity of R to the new physics cross sections, and the slope of the upward flux as a function of nadir angle, we see that a signal of low scale gravity models would stand out clearly.

4 Conclusions:

KM^3 detectors have been planned primarily as “neutrino telescopes”. However our study indicates that KM^3 will also provide vigorous new exploration of fundamental questions in ultra-high energy physics. Extra dimension, low scale gravity models show an observable impact on the signature of neutrino events in the KM^3 detectors such as the currently running RICE detector and the ICECUBE detector, which is in the R & D stage. Of the “strong

gravity” effects we looked at, the black hole formation cross section and the extrapolation of the small q^2 , part of $\sigma^{\nu N}$ from the $s < M^2$ to $s \gg M^2$ within the ADD model yield the largest detectable effects.

While some observables are somewhat sensitive to the number of dimensions, n , most are *quite sensitive* to the value of the scale of gravity M . If M is 1-2 TeV, the enhanced $\sigma^{\nu N}$ creates a clearly recognizable signature, with the “neutral-to- charged” event ratio still showing new physics effects at $M = 5$ TeV. The ratio R of upcoming to down-going events is a powerful diagnostic, capable of discriminating between models if fluxes are large enough to produce a significant number of upcoming events. In the entire analysis, we emphasized that the regeneration of neutrino upcoming flux due to neutrinos scattering down from higher to lower energies is a crucial feature of the gravity-induced neutral current interactions. This is a general and important feature of our work presented here.

Considering only down-coming events, we propose that the fraction of neutral current type events, those with hadronic showers and no leading charged lepton, provides a probe of new interactions. In particular, event signatures arising from a *dominant* component of eikonized graviton exchange or of black hole production as occur in low scale gravity models, would have *no standard physics explanation*, and would point the way toward physics beyond the Standard Model if observed. There is every reason to believe that the neutral-to-charged current ratio can be extracted from upcoming facilities well enough to make a practical signal. In particular, determining the ratio of events with a muon, to those making an isolated shower, is certainly feasible with a combination of AMANDA/ICECUBE and RICE technology. The striking behavior of the neutral current-to-charged current ratio is shown in Fig. 3.

Finally, the shape and *slope* of the angular distribution, Fig. 6, is found to have good discriminating power. The shape does not depend at all on the overall normalization of the flux. Moreover the slopes differ substantially right in the regime of maximum detectable flux, near $\pi/2$ nadir angle, and is ideal for comparing low scale gravity models to the Standard Model. Whether or not extra-dimension models as currently envisaged survive, the angular distribution can severely test the neutrino physics of the Standard Model, possibly strongly bounding or even discovering new physics, as soon as data becomes available.

Acknowledgements: P. Jain thanks the University of Kansas College of

Arts and Sciences and Department of Physics and Astronomy for hospitality and support in the course of this work. This research was supported in part by the U.S. Department of Energy under grant number DE-FG03-98ER41079. We used computational facilities of the Kansas Center for Advanced Scientific Computing for part of this work.

References

- [1] N. Arkani-Hamed, S. Dimopoulos and G. Dvali, Phys. Lett. B **429**, 263 (1998).
- [2] L. Randall and R. Sundrum, Phys. Rev. Lett. **83**, 3370 (1999).
- [3] S. Nussinov and R. Shrock, Phys. Rev. D **59**, 105002 (1999).
- [4] G. Domokos and S. Kovesi-Domokos, Phys. Rev. Lett. **82**, 1366 (1999).
- [5] P. Jain, D. McKay, S. Panda and J. Ralston, Phys. Lett. B **484**, 267 (2000).
- [6] S. Nussinov and R. Shrock, Phys. Rev. D **64**, 047702 (2001); A. Jain, P. Jain, D. McKay and J. Ralston, hep-ph/0011310, Int. Jour. of Mod. Phys. A **17**, 533 (2002); C. Tyler, A. Olinto and G. Sigl, Phys. Rev. D **63**, 55001 (2001); L. Anchordoqui, H. Goldberg, T. McCauley, T. Paul, S. Reucroft and J. Swain, Phys. Rev. D **63**, 124009 (2001); M. Kachelriess and M. Plumacher, Phys. Rev. E **62** (2000).
- [7] J. Feng and A. Shapere, Phys. Rev. Lett. **88**, 021303 (2002); A. Anchordoqui and H. Goldberg, Phys. Rev. D **65**, 047502 (2002).
- [8] R. Emparan, M. Masip and R. Rattazzi, Phys. Rev. D **65**, 064023 (2002).
- [9] A. Ringwald and H. Tu, Phys. Lett. B **525**, 135 (2002).
- [10] L. Anchordoqui, J. Feng, H. Goldberg and A. Shapere, Phys. Rev. D **65**, 124027 (2002).
- [11] M. Kowalski, A. Ringwald and H. Tu, Phys. Lett. B **529** 1 (2002).

- [12] K. Greisen, Phys. Rev. Lett. **16**, 748 (1966); G. Zatsepin and V. Kuzmin, Pis'ma Zh. Eksp. Teor. Fiz. **4**, 114 (1966) [JETP. Lett. **4**, 78 (1966)].
- [13] J. Alvarez-Muñiz, F. Halzen, T. Han and D. Hooper, Phys. Rev. Lett. **88**, 021301 (2002).
- [14] J. Alvarez-Muñiz, J. Feng, F. Halzen, T. Han and D. Hooper, Phys Rev. D **65**, 124015 (2002).
- [15] S. Yoshida *et al.* [AGASA Collaboration], in Proc. 27th International Cosmic Ray Conference, Hamburg, Germany, 2001, Vol. 3, p 1142; D. Zavrtanik [AUGER Collaboration], Nucl. Phys. Proc. Suppl. **85**, 324 (2000); D. Bird *et al.* [Fly's Eye Collaboration], Ap. J. **441**, 151 (1995); J. Matthews *et al.* [HiRes Collaboration], in Proc. 27th International Cosmic Ray Conference, Hamburg, Germany, 2001, Vol. 1, p. 350; M. Lawrence, R. Reid and A. Watson, J. Phys. G **17**, 733 (1991).
- [16] F. Halzen *et al.* [AMANDA Collaboration] in Proceedings of the 26th International Cosmic Ray Conference (ICRC 99), Salt Lake City, 17-25 Aug. 1999, B. L. Dingus, D. B. Kieda, M. H. Salamon (Eds.), (AIP, 2000) pp. 428-431. T. Montaruli [ANTARES Collaboration], hep-ex/0201009; V. Balkanov *et al.*, Baikal Collaboration], astro-ph/0112446; P. Greider [NESTOR Collaboration], Nucl. Phys. Proc. Suppl. **97**, 105 (2000); I. Kravchenko *et al.* [RICE Collaboration], astro-ph/0112372; The ICECUBE Project, <http://www.ssec.wisc.edu/a3ri/icecube>.
- [17] F. Halzen *et al.* [AMANDA Collaboration] in Proceedings of the 26th International Cosmic Ray Conference (ICRC 99), Salt Lake City, 17-25 Aug. 1999, B. L. Dingus, D. B. Kieda, M. H. Salamon (Eds.), (AIP, 2000) pp. 428-431.
- [18] I. Kravchenko *et al.* [RICE Collaboration], astro-ph/0112372.
- [19] I. Kravchenko *et al.* [RICE Collaboration], astro-ph/0206371.
- [20] The ICECUBE Project, <http://www.ssec.wisc.edu/a3ri/icecube>.

- [21] V. Berezhinskii, A. Gazizov, G. Zatsepin and I. Rozenal, *Yad. Fiz.* **43**, 637 (1986); *Sov. J. Nucl. Phys.* **43**, 406 (1986).
- [22] For an application in the context of the present discussion, see G. M. Frichter, J. P. Ralston and D. W. McKay, *Phys. Rev. D* **53**, 1684 (1996).
- [23] R. Emparan, *Phys. Rev. D* **64**, 0204025 (2001).
- [24] G. Giudice, R. Rattazzi and J. Wells, *Nucl. Phys. B* **630**, 293 (2002).
- [25] I. Antoniadis, N. Arkani-Hamed, S. Dimopoulos and G. Dvali, *Phys. Lett. B* **463**, 257 (1998).
- [26] S. Cullen, M. Perelstein and M. Peskin, *Phys. Rev. D* **62**, 055012.
- [27] E. Dudas and J. Mourad, *Nucl Phys. B* **575**, 3 (2000); R. Cornet, J. Illana and M. Masip, *Phys. Rev. Lett.* **86**, 4235 (2001).
- [28] S. Dimopoulos and R. Emparan, *Phys. Lett. B* **526**, 393 (2002).
- [29] S. Dimopoulos and G. Landsberg, *Phys. Rev. Lett.* **87**, 161602 (2001); S. Giddings and S. Thomas, *Phys. Rev. D* **65**, 056010 (2002).
- [30] E-J. Ahn, M. Cavaglia and A. Olinto, hep-th/0201042; P. Jain, S. Kar, S. Panda and J. Ralston, hep-ph/0201232.
- [31] H.L. Lai et al., *Phys. Rev. D.* **55**, 1280 (1997).
- [32] M. Voloshin, *Phys. Lett. B* **518**, 137 (2001); *ibid* **524**, 376 (2002).
- [33] J. Ralston, “Quantum Suppression of Black-Hole Formation in High Energy Scattering”, (unpublished).
- [34] S. Giddings, hep-ph/0110127
- [35] T. Rizzo, *JHEP* **0202**, 011 (2002).
- [36] G. Pásztor and T. Rizzo, hep-ph/0112054.
- [37] G. 't Hooft, *Phys. Lett. B*, **198**, 61 (1987).
- [38] J.Hewett and M Spiropulu, hep-ph/0205106.

- [39] F. W. Stecker, C. Done, M. Salamon and P. Sommers, Phys. Rev. Lett. **66**, 2697 (1991); erratum Phys. Rev. Lett. **69**, 2738 (1992).
- [40] J. Bahcall and E. Waxman, Phys. Rev. D **64**, 023002 (2001).
- [41] J. Beacom, P. Crotty and E. Kolb, astro-ph/0111482.

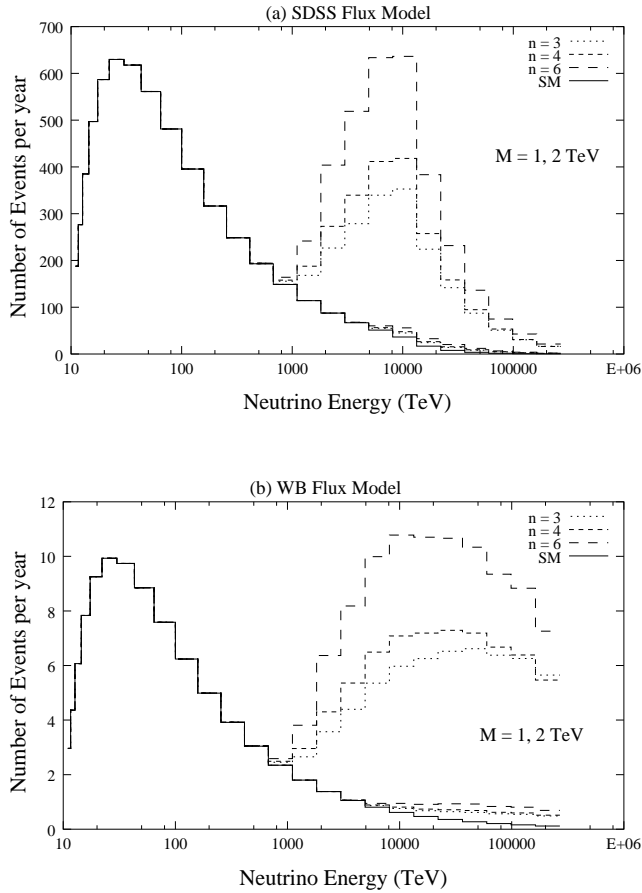


Figure 2: The downwards event rate per cubic kilometer per year within the Standard Model (SM) and in the ADD model for the fundamental scale $M = 1, 2$ TeV and for the number of extra dimensions, $n = 3, 4, 6$ using (a) the SDSS flux model and (b) the WB flux model. The solid line shows the Standard Model prediction alone. The long dashed, dotted and short dashed curves show the predictions of the neutral current graviton exchange within the ADD model plus geometric, black hole cross sections, and including the SM contribution. The upper and lower histograms correspond to the $M = 1, 2$ TeV choices respectively. The new physics contributions are insignificant below 1 PeV, where their contribution above the SM is not visible on this scale.

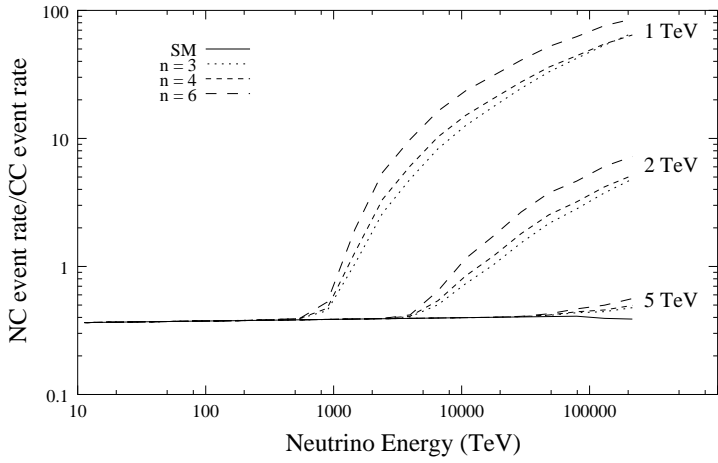


Figure 3: The ratio of neutral current type events to SM charged current events as a function of neutrino energy for $n = 3, 4$ and 6 and for $M = 1, 2,$ and 5 TeV. Only the downward events are included in this plot. The neutral current type interactions, in the sense used here, are dominated by the black hole and eikonal components of the low scale gravity amplitude above the scale of gravity.

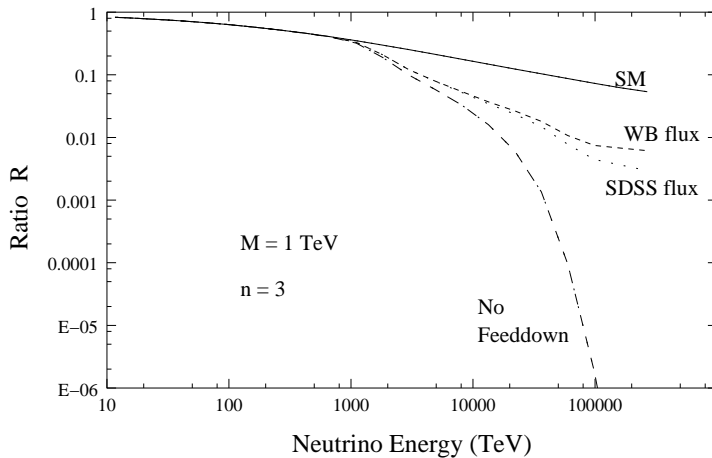


Figure 4: The contribution of the regeneration term to the ratio R of the upwards and downwards flux within the ADD plus geometric black hole production model with the fundamental scale $M = 1$ TeV and for the number of extra dimensions equal to 3. The long dashed line (flux from [39]) and short dashed line (flux from [40]) predict nearly the same R as a function of energy for the full calculation, including the regeneration term. Ignoring the regeneration of flux, one gets the lowest curve, identical for both flux models. The regeneration term has a profound effect on the up-to-down flux ratio R due to the large, gravity driven neutral current cross section. Standard model prediction, the solid line, is also shown and it is the same for both flux assumptions.

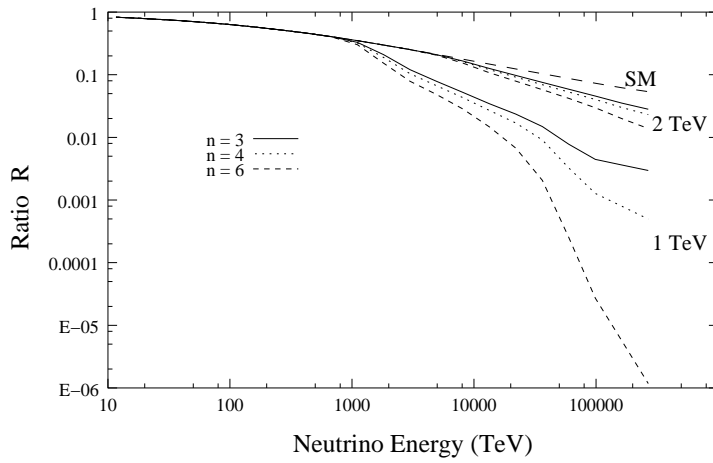


Figure 5: The ratio R as a function of neutrino energy for the fundamental scale $M = 1, 2$ TeV and for the number of extra dimensions 3 (solid curves), 4 (dotted curves) and 6 (dashed curves). The Standard model (SM) prediction is also shown.

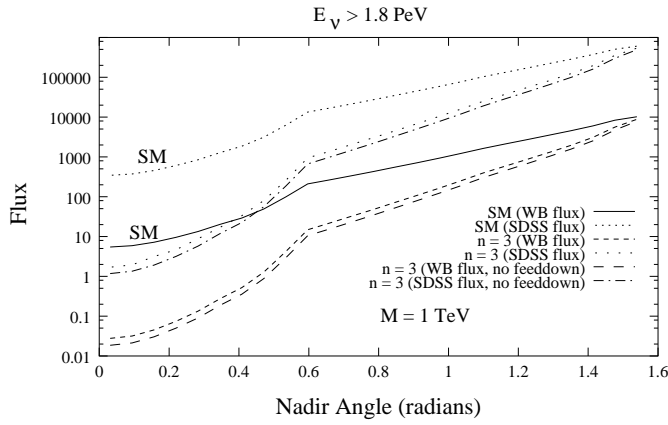


Figure 6: The angular dependence of the upwards flux for the fundamental scale $M = 1, 2$ TeV and for the number of extra dimensions, $n = 3, 4, 6$. The Standard model (SM) prediction is also shown. Only neutrinos with energy $E_\nu > 1.8$ PeV are considered. The $M = 2$ TeV results are indistinguishable from the Standard Model, but the R value is different because downward event rate is larger in the $M=2$ low scale gravity model (see Fig.2).